Korean J. Chem. Eng., **30**(3), 587-592 (2013)
DOI: 10.1007/s11814-012-0204-z

Glycerol steam reforming over Ni/γ-Al_2O_3 catalysts modified by metal oxides

Zun-Yu Huang, Cheng-Hua Xu†, Chuan-Qi Liu, Hui-Wen Xiao, Jun Chen, Yong-Xiang Zhang, and Ya-Cong Lei

Air Environmental Modeling and Pollution Controlling Key Laboratory of Sichuan Higher Education Institutes, Chengdu University of Information Technology, Chengdu 610225, China
(*Received 10 August 2012 • accepted 19 November 2012*)

Abstract−The metal oxides modified Ni/γ-Al_2O_3 catalysts for glycerol steam reforming were prepared by impregnation. Characterization results of fresh catalysts indicated that the molybdates modification abated the acidity and the stronger metal-support interaction of Ni/γ-Al_2O_3 catalysts, leading to a stable catalytic activity. Especially, NiMoLa-CaMg/γ-Al_2O_3 (NiMoLa/CMA) catalyst exhibited no deactivation along with glycerol complete conversion to stable gaseous products containing 69% H_2, 20% CO and 10% CO_2 during time-on-stream of 42 h. TPO of spent Ni/γ-Al_2O_3 catalysts modified by different components showed that the carbon deposit on acidic sites and $NiAl_2O_4$ species led to catalysts deactivation. A lower reforming temperature and a higher LHSV and glycerol content were helpful to the production of syngas from GSR over NiMoLa/CMA; the reverse conditions would improve the formation of H_2.

Key words: Glycerol, Steam Reforming, Syngas, Hydrogen

INTRODUCTION

With increasing production of biodiesel, a great deal of glycerol will be by-produced during biodiesel manufacturing by transesterification of vegetable oils or animal fats. Therefore, glycerol utilization is a very important subject, and much attention has already been focused on this field. For examples, glycerol can be used for the production of 1,2-propanol, 1,3-propanol and other important chemical intermediates [1-3]. As a kind of oxygenated hydrocarbon, glycerol can also be catalytically converted to H_2 and syngas, which are applied in fuel cells [4] and the Fischer-Tropsch synthesis [5,6].

It was reported that the noble metal catalysts [7-12] such as Pt, Pd and Ru exhibited a high catalytic activity; however, the conventional reforming catalysts such as Ni/Al_2O_3 gave a low activity and poor catalytic stability due to coke formation in glycerol steam reforming (GSR) [8,10]. Some researchers [10] found that the addition of a small amount of noble metal could improve the catalytic properties of Ni-based catalysts in GSR. However, it could also increase the catalyst cost. Other researchers [13-15] found that the deactivation of Ni-based catalysts in catalytic steam reforming of other hydrocarbons was also mainly due to the carbon deposit occurred on the acidic sites over catalysts surface, which could be overcome by adding alkaline elements such as K, Ca or Mg. Additionally, some studies [16-19] indicated that the modification of Mo oxides could improve the stability of Ni/Al_2O_3 catalyst with a high activity for the reforming of other hydrocarbons such as CH_4 and ethanol so on.

Therefore, the present work first adopts alkaline earth metal elements such as Ca or Mg modified Ni/γ-Al_2O_3 catalyst with a low cost in order to reduce catalysts acidic sites, and further modifies the obtained catalysts by adding the other transition metal elements such as La, Ce, Y, Zr or Mo in order to improve its catalytic stability in GSR. The functions of the introduced metals in the corresponding catalysts are investigated through the characterization by using XRD, H_2-TPR and NH_3-TPD. The catalytic properties of the modified Ni/γ-Al_2O_3 catalysts are compared and the carbon deposit over the spent catalyst is tested by TPO. Additionally, the effects of reforming parameters on GSR over the key catalysts are also investigated in detail.

EXPERIMENTAL

1. Catalysts Preparation

Ni/Al_2O_3 catalysts modified by metal oxides were prepared by the incipient wetness impregnation. Typically, the dried commercial γ-Al_2O_3 (S_{BET}=210 $m^2 \cdot g^{-1}$, particle size 0.8-1.2 mm) was first impregnated in the aqueous solution containing $Ca(NO_3)_2 \cdot 4H_2O$ and $Mg(NO_3)_2 \cdot 6H_2O$ at room temperature for 4 h, and then dried overnight at 100 °C and calcined at 800 °C for 6 h in air. Thus, the γ-Al_2O_3 supports (CMA) modified by Ca and Mg oxides were obtained. The further modification of supports CMA with the other metal elements such as La, Ce, Y or Zr was also carried out by using the corresponding nitrates as precursors according to the similar procedure, Mo precursor was $(NH_4)_6Mo_7O_{24} \cdot 4H_2O$. After the modification, the Ni loading was carried out by the above method using $Ni(NO_3)_2 \cdot 6H_2O$ as precursor. The obtained catalysts are denoted as Ni*M*/CMA, wherein *M* represents the modified metal oxides except Ca and Mg. The introduced amounts of modified metal oxides and Ni were 3 wt% and 10 wt%, respectively.

2. Catalysts Characterization

The Ni actual contents in prepared catalysts were determined by using a Shimadzu XRF-1800 X-ray fluorescence (XRF) spectrometer. The BET specific surface areas (S_{BET}), pore volume and pore diameter of catalysts were measured by the N_2 adsorption-desorption isotherms at −196 °C using an SSA-4200 micromeritics instrument (Builder Co., Beijing). Powder X-ray diffraction (XRD) analyses were carried out to verify the crystalline structure of the pre-

†To whom correspondence should be addressed.
E-mail: xch@cuit.edu.cn

pared catalysts, and these experiments were performed on a DX-2700 powder diffractometer (Dandong, China) operated at 30 kV and 20 mA, using Cu $K\alpha$ radiation. Temperature-programmed reduction by H_2 (TPR). temperature-programmed desorption of ammonia (NH_3-TPD) and Temperature-programmed oxidation (TPO) were performed with a TP-5080 adsorption instrument (Tianjing, China) equipped with a thermal conductivity detector (TCD). In a typical TPR experiment, 100 mg of sample placed in a quartz tube was first degassed under a 30 ml·min^{-1} of N_2 flow at 300 °C for 30 min. After cooling to about 40 °C in N_2, the sample was heated from room temperature to 950 °C under a 30 ml·min^{-1} of 5% H_2-N_2 mixture gas, and the heating rate was 10 °C·min^{-1}. For NH_3-TPD, 200 mg of catalysts were pretreated in He at 400 °C for 30 min, and then NH_3 adsorption was carried in 30 ml·min^{-1} of He carrier gas containing 10 vol% NH_3 for another 30 min. Subsequently the physisorbed NH_3 molecules over samples were removed by He flow for 2 h. The TPD of the obtained sample was heated in 30 ml·min^{-1} of He at a rate of 10 °C·min^{-1} from 50 °C to 700 °C for NH_3 desorption. For TPO, 200 mg spent catalysts were introduced into a quartz tube and dried at 150 °C to remove physisorbed water and then cooled to room temperature in N_2. The TPO measurements were performed under a flow of 5% O_2-N_2 mixture (30 ml·min^{-1}) from room temperature to 700 °C at a heating rate of 10 °C·min^{-1}. The O_2 consumption and the formation of CO/CO_2 were generally measured with TCD.

3. Glycerol Steam Reforming

GSR was conducted in a vertical fixed-bed quartz reactor (20 mm diameter and 600 mm length). Prior to the catalytic test, 12 g catalysts (apparent volume about 15 ml) were reduced in a 60 ml·min^{-1} of H_2 flow at 850 °C for 2 h. Then the temperature was adjusted to 750 °C and 100 ml·min^{-1} of N_2 as balance carrier gas was introduced. After the residual H_2 was completely removed, 35 wt% of glycerol aqueous solution was injected by a micro-pump at a flow rate of 42 ml·h^{-1} to start the reaction measurements. Behind the reactor outlet the reaction mixture was cooled by ice-water bath and separated. The volume of the produced gaseous mixture was monitored by wet type gas flowmeter, and the composition of gas products including H_2, CO, CO_2 and CH_4 was analyzed by on-line gas chromatograph (GC-2000, Chongqing, China) equipped with a TDX-01 (carbon molecular sieves, 3 m×3 mm) packed column and TCD. Glycerol conversion was calculated according to the GC analysis of the collected liquid products on another GC-2000 gas chromatograph equipped with a KB-Wax capillary column (30 m×0.32 mm×0.5 μm, Kromat Co., USA) and a flame ionization detector (FID). For the investigation on the effect of reforming parameters, all conditions were unchanged except for the tested one.

RESULTS AND DISCUSSION

1. Catalysts Characterization

The N_2 adsorption-desorption measurement results of the prepared Ni-based catalysts show that the surface area decreases with increases in metal loading. It may be attributable to the pore blockage by the introduced metal oxides. Additionally, the total pore volume and average pore diameter of the catalysts seem to also give a decreasing trend after loading the modified metal oxides.

XRD results of Ni/γ-Al_2O_3 catalysts modified by metal oxides

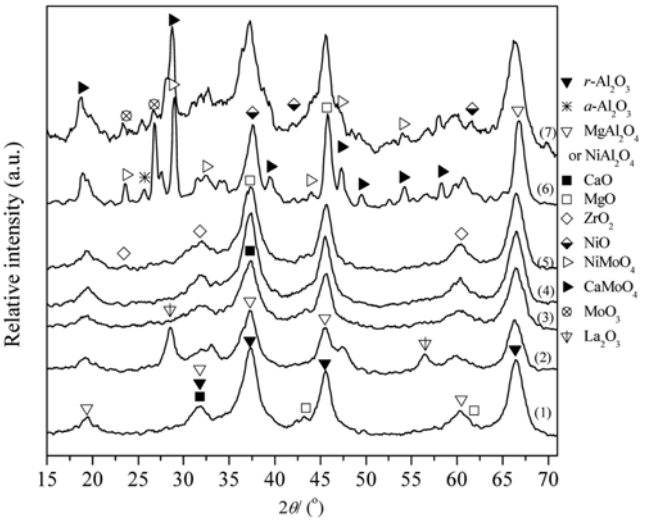

Fig. 1. XRD patterns of (1) Ni/CMA, (2) NiLa/CMA, (3) NiCe/CMA, (4) NiY/CMA, (5) NiZr/CMA, (6) NiMo/CMA, and (7) NiMoLa/CMA.

(Fig. 1) show that the introduced metal elements except for Mo mainly exist in the form of corresponding oxides on the support surface. Fig. 1 shows that XRD pattern of Ni/γ-Al_2O_3 modified by Y and Ce (curves (3) and (4)) does not exhibit the characteristic signal of the corresponding oxides, and the introduction of La gives rise to the formation of La_2O_3 (see curve (2)). Although two typical characteristic peaks for NiO species (Pdf. 2-1216) at 2θ=37.5° and 43° are very difficult to distinguish with those of γ-Al_2O_3, $MgAl_2O_4$, another NiO characteristic peak at 2θ=62° cannot also be clearly observed for those catalysts except for NiMo/CMA and NiMoLa/CMA. It indicates that the bivalent metals such as Ca^{2+}, Mg^{2+} and Ni^{2+} can easily interact with γ-Al_2O_3 to spinel phase (Pdf. 1-1157 and 1-1299), which is possibly due to the stronger metal-support interaction (SMSI) in Ni/γ-Al_2O_3 catalysts [17]. For NiMo/CMA,

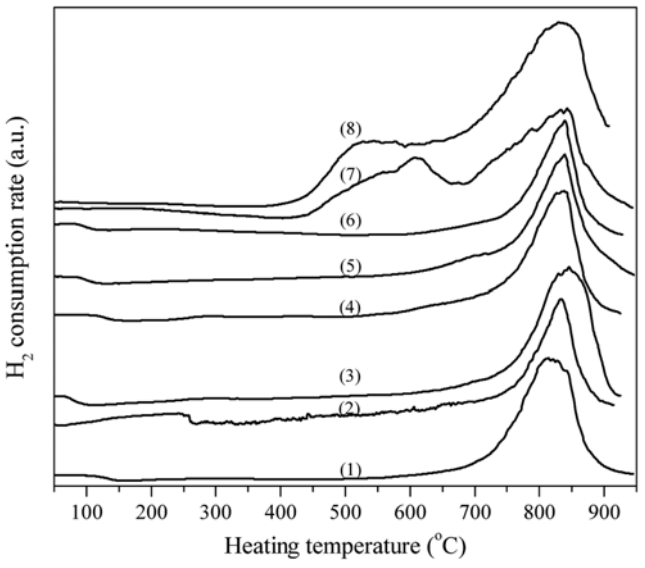

Fig. 2. H_2-TPR profiles for catalysts: (1) Ni/γ-Al_2O_3, (2) Ni/CMA, (3) NiLa/CMA, (4) NiCe/CMA, (5) NiY/CMA, (6) NiZr/CMA, (7) NiMo/CMA and (8) NiMoLa/CMA.

the introduction of Mo into Ni/γ-Al_2O_3 consisting of Ca and Mg leads to the formation of $CaMoO_4$ and $MgMoO_4$ (Pdf. 77-2238) or $NiMoO_4$ (Pdf. 18-879) besides MoO_3 (Pdf. 76-1003) species [18, 19] and α-Al_2O_3 (Pdf. 11-661). However, NiMoLa/CMA has less $NiMoO_4$ and MoO_3 due to the presence of La (compare curves (6) and (7)). Moreover, the XRD patterns of NiMo/CMA and NiMoLa/CMA exhibit a weak NiO characteristic peak at 2θ=62°, which implies that the simultaneous introduction of Mo and La into Ni/CMA leads to the formation of more surface NiO species. It is probably because the formation of α-Al_2O_3 and the coexistence of La_2O_3, MoO_3, molybdates (such as $CaMoO_4$, $MgMoO_4$) weaken SMSI between Ni and support [11,17].

In the present work, H_2-TPR is introduced to investigate SMSI between Ni species and support in the mentioned-above catalysts.

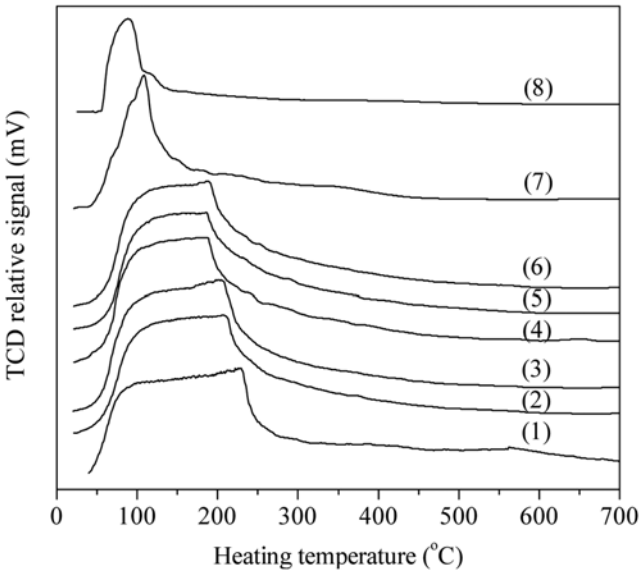

Fig. 3. NH_3-TPD curves for catalysts: (1) Ni/γ-Al_2O_3, (2) Ni/CMA, (3) NiLa/CMA, (4) NiCe/CMA, (5) NiY/CMA, (6) NiZr/CMA, (7) NiMo/CMA and (8) NiMoLa/CMA.

The results (Fig. 2) show that Ni/γ-Al_2O_3 catalyst and those modified by Ca-Mg, La-Ca-Mg, Ce-Ca-Mg, Y-Ca-Mg and Zr-Ca-Mg only exhibit a single H_2 consumption peak maximum above 810 °C, attributed to the reduction of Ni^{2+} species located in $NiAl_2O_4$ spinel phase [17,18] detected by XRD (Fig. 1). For the Mo-modified Ni/CMA catalysts, the TPR peak at about 810 °C is widened (see curves (7) and (8) in Fig. 2), which is probably induced by the reduction of Mo^{6+} to Mo^{4+} or Ni^{2+} to Ni^0 in $NiMoO_4$ [17]. Moreover, both NiMo/CMA and NiMoLa/CMA exhibit a new low temperature TPR peak at about 630 °C and 510 °C, respectively. The modification of Mo and La gives rise to the formation of more surface NiO active species.

$$C_3H_8O_3 \longrightarrow 3CO + 4H_2 \quad (1)$$
$$CO + H_2O \longrightarrow CO_2 + H_2 \quad (2)$$
$$CO + 3H_2 \longrightarrow CH_4 + H_2O \quad (3)$$
$$CO_2 + 4H_2 \longrightarrow CH_4 + 2H_2O \quad (4)$$

Scheme 1. The possible reactions involved in GSR.

Table 1. The Ni content, BET surface area, pore volume and pore diameter of prepared catalysts

Catalysts	Ni (wt%)[a]	S_{BET}[b]	Pore volume (cm/g)[b]	Pore diameter (nm)[b]
Ni/γ-Al_2O_3	9.8	181.3	0.22	3.02
NiCa/γ-Al_2O_3	9.7	183.4	0.21	2.86
NiMg/γ-Al_2O_3	9.7	173.8	0.20	2.45
Ni/CMA	9.6	170.2	0.19	2.57
NiLa/CMA	9.7	158.3	0.17	2.54
NiCe/CMA	9.6	148.9	0.18	2.11
NiY/CMA	9.6	143.8	0.18	2.16
NiZr/CMA	9.7	124.5	0.16	2.26
NiMo/CMA	9.6	115.5	0.15	2.21
NiMoLa/CMA	9.5	96.1	0.15	2.23

[a]Derived from XRF

[b]Derived from N_2 adsorption/desorption

Table 2. Catalytic properties of different catalysts in GSR[a]

Catalysts	Glycerol conversion (mol%)[b]	C conversion to gaseous products[c]	Gas total volume produced in 2 h (L)	Production ratio of gas (L/g_{Gly})[d]	Gaseous products distribution (mol%)			
					H_2	CO	CO_2	CH_4
Ni/γ-Al_2O_3	63.86	54.06	34.381	1.169	74.07	6.40	17.89	1.64
NiCa/γ-Al_2O_3	90.65	60.08	38.214	1.300	74.81	6.55	16.94	1.70
NiMg/γ-Al_2O_3	83.69	58.05	36.921	1.256	74.78	6.40	16.61	2.21
Ni/CMA	84.59	68.43	43.523	1.480	67.92	9.19	20.57	2.33
NiLa/CMA	83.97	66.21	42.107	1.432	71.83	8.14	17.32	2.71
NiCe/CMA	48.15	29.64	18.851	0.641	69.02	10.35	16.49	4.14
NiY/CMA	67.32	43.44	27.631	0.940	68.55	9.95	17.40	4.10
NiZr/CMA	63.14	38.07	24.215	0.824	68.16	9.44	19.16	3.24
NiMo/CMA	93.40	93.03	57.258	1.948	65.16	10.55	19.90	4.39
NiMoLa/CMA	99.12	99.08	60.018	1.985	63.23	17.68	14.13	4.95

[a]15 ml catalyst, temperature 750 °C, 42 $ml \cdot h^{-1}$ of 35% glycerol aqueous solution, 100 $ml \cdot h^{-1}$ of N_2 as balance gas

[b]Glycerol conversion is calculated by the GC analysis of liquid mixture collected after reaction 2 h

[c]The data are calculated by C balance

[d]The total volume of produced gas per gram of converted glycerol

It further indicates that the presence of Mo species is able to weaken SMSI between Ni and support, leading to the increase of surface Ni active species. This SMSI can be further weakened by the simultaneous modification of Mo and La, because the TPR peak of NiMoLa/CMA at below 630 °C shifts to a lower temperature (curve (8) in Fig. 2).

NH_3-TPD profiles (Fig. 3) of the Ni/CMA catalysts modified by other metal oxides indicate that the introduction of rare earth and alkaline earth metals makes the NH_3 desorption peak of Ni/γ-Al_2O_3 catalysts narrow and shift to a low temperature. It shows that the modification of these metal oxides can also decrease the acidity of Ni/γ-Al_2O_3 surface in some extent. Moreover, the modification of Mo and Mo-La complex oxides can further decrease the acidity of catalysts surface, which is perhaps from the interaction of molybdate anions with hydroxyl groups on alumina surface during the catalysts' calcination [20]. This interaction can also lead to a decreasing SMSI between Ni and support γ-Al_2O_3.

2. Catalytic Reforming and Catalyst Stability

During GSR, the thermal reforming of glycerol firstly occurs, which leads to the formation of H_2 and CO mixture gas with a theoretical H_2/CO ratio of 4 : 3 as described in Eq. (1). The produced CO can be converted to CO_2 and H_2 through water-gas shift reaction (Eq. (2)), which is able to raise the H_2/CO ratio and amount of gas products. Additionally, the methanation of CO or CO_2 to CH_4 is possibly involved in GSR [7,11,21]. Therefore, the produced main gaseous products include H_2, CO, CO_2 and CH_4; all possible reactions are described in Scheme 1.

The catalytic results (Table 2) indicate that all Ni/γ-Al_2O_3 catalysts exhibit catalytic activity on the water-gas shift reaction of CO to CO_2 and methanation of CO or CO_2 during GSR. From glycerol conversion during time-on-stream of 2 h over Ni/γ-Al_2O_3 catalysts modified by different metal oxides, it is found that the modification of Ce-Ca-Mg, Y-Ca-Mg and Zr-Ca-Mg oxides can't lead to an obvious increase in the catalytic activity of Ni/γ-Al_2O_3 for GSR. However, Ni/γ-Al_2O_3 catalysts modified by Mo-La-Ca-Mg, Mo-Ca-Mg, La-Ca-Mg, Ca-Mg, Ca and Mg give a higher glycerol conversion (>83%). From Table 2, it can also be found that the converted glyc-

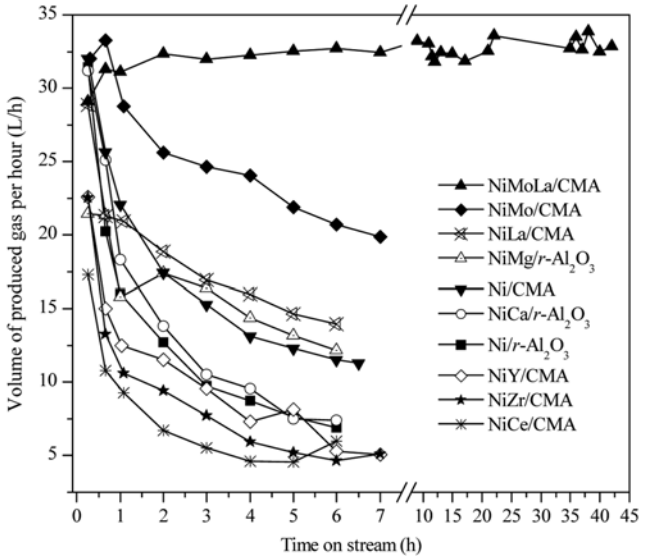

Fig. 4. Produced rate of gas with stream time over different catalysts in GSR. Conditions: 15 ml catalyst, temperature 750 °C, 42 ml·h^{-1} of 35 wt% glycerol aqueous solution and 100 ml·h^{-1} N_2 as balance gas.

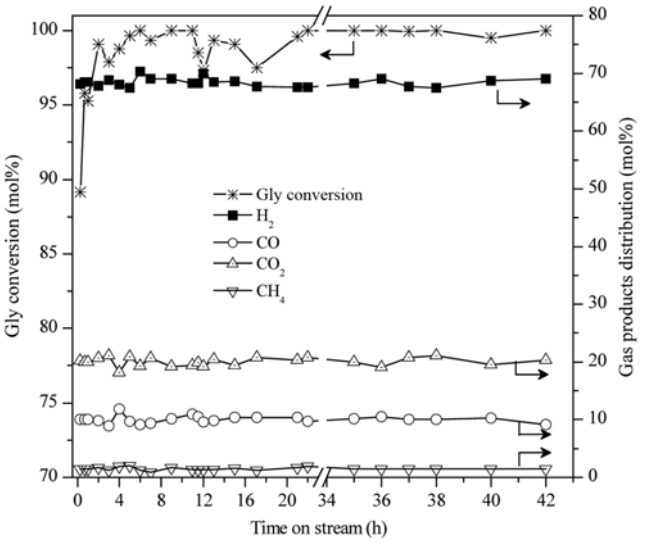

Fig. 5. Catalytic stability of NiMoLa/CMA catalyst in GSR. Conditions: 15 ml catalyst, temperature 750 °C, feed rate of 35% glycerol aqueous solution 42 ml·h^{-1} and 100 ml·h^{-1} N_2 as balance gas.

Table 3. Carbon deposit over the spent catalysts in GSR[a]

Spent catalysts	Time on stream (h)	Total carbon deposit (mmol·g$^{-1}_{cat}$)[b]	Temperature at max TPO peak (°C)	Average rate of carbon deposit (mmol·g$^{-1}_{cat}$·h^{-1})
Ni/γ-Al_2O_3	6	11.71	540	1.952
NiCa/γ-Al_2O_3	6	8.72	497	1.453
NiCe/CMA	6	17.86	488	2.976
NiZr/CMA	7	15.81	499	2.259
NiY/CMA	7	15.53	478	2.219
Ni/CMA	6.5	9.21	515	1.417
NiLa/CMA	6	3.62	471	0.603
NiMo/CMA	7	0.72	498	0.103
NiMoLa/CMA	42	0.17	497	0.004

[a]15 ml catalyst, temperature 750 °C, 42 ml·h^{-1} of 35% glycerol aqueous solution and 100 ml·h^{-1} of N_2 as balance gas
[b]The data are obtained according to TPO analysis

erol can't completely produce gaseous products over catalysts except for NiMoLa/CMA and NiMo/CMA. GC analysis shows that a part of converted glycerol produces acrolein, dihydroxy acetone, hydroxyacetone, formaldehyde and acetaldehyde so on through thermal decomposition, dehydrogenation and dehydration over these catalysts [22]. It is possibly because the addition of these metal oxides exhibits a poor effect for the improvement in the reducibility of Ni species through decreasing SMSI of Ni/γ-Al_2O_3, resulting in a weak activity for the C-C bonds cleavage of glycerol. However, both catalysts modified by Mo-La-Ca-Mg and Mo-Ca-Mg can make the converted glycerol to completely form gaseous products (above 93%) and give a higher gas production capacity. According to the above H_2-TPR and XRD results, it can be concluded that the excellent catalytic property of both catalysts is due to the decrease on SMSI between Ni and support resulted from the simultaneous presence of alkaline oxides, La_2O_3 and MoOx species (such as MoO_3, $CaMoO_4$ and $MgMoO_4$). Additionally, the electronic structure of active Ni species can be modified through the electron transfer from MoOx species to Ni [18], which also improves GSR.

The rates of gas production with time-on-stream over different catalysts (Fig. 4) show that the catalytic stability of catalysts in GSR decreases in the following order: NiMoLa/CMA>NiMo/CMA>NiLa/CMA>NiMg/γ-Al_2O_3>Ni/CMA>NiCa/γ-Al_2O_3>Ni/γ-Al_2O_3>NiY/CMA>NiZr/CMA>NiCe/CMA. NiMoLa/CMA exhibits no deactivation (glycerol conversion ~99%) along with stable gaseous products consisting of 69% H_2, 20% CO and 10% CO_2 (Fig. 5), respectively.

TPO results of the spent catalysts (Table 3) show that Ni/γ-Al_2O_3 catalysts modified by Mo-La-Ca-Mg and Mo-Ca-Mg give the least carbon deposit. It indicates that the deactivation of Ni/γ-Al_2O_3 catalysts in GSR mainly results from the carbon deposit on catalysts surface. According to the present results and the previous studies [10, 19,23] on the reforming of other oxygenated hydrocarbons, carbon deposit possibly occurs on the acidic sites of support and Ni metal located in $NiAl_2O_4$ species. The decrease in acidity of catalyst surface and SMSI between Ni and γ-Al_2O_3 can inhibit the carbon deposit, leading to an excellent catalytic stability of Ni-based catalysts in GSR.

3. Effect of Reforming Parameters

In the present work, the effects of reforming parameters on the catalytic property of the Ni/γ-Al_2O_3 catalyst modified by Mo-La-Ca-Mg (NiMoLa/CMA) with an excellent catalytic stability are further investigated. From Fig. 6(a), the gas volume of gas produced per gram glycerol in GSR over NiMoLa/CMA rapidly increases with an increasing reforming temperature, because the higher temperature can improve the water-gas shift reaction of CO to CO_2 (Eq. (2) in Scheme 1) along with the production of more H_2. However, the reforming temperature seems to have no obvious effect on the methanation of CO or CO_2. From Fig. 6(a), a lower reforming temperature is helpful to the GSR to syngas (H_2/CO=2.01 at 600 °C). At a higher temperature (800 °C), the water-gas shift reaction can promote the conversion of CO to CO_2 and H_2, which is advantageous to production of H_2 in GSR.

The effect of feed rate of glycerol aqueous solution on GSR over NiMoLa/CMA (Fig. 6(b)) shows that the conversion of glycerol to gas products, and CO_2 content in gaseous product decrease with the increasing liquid hourly space velocity (LHSV) to some extent;

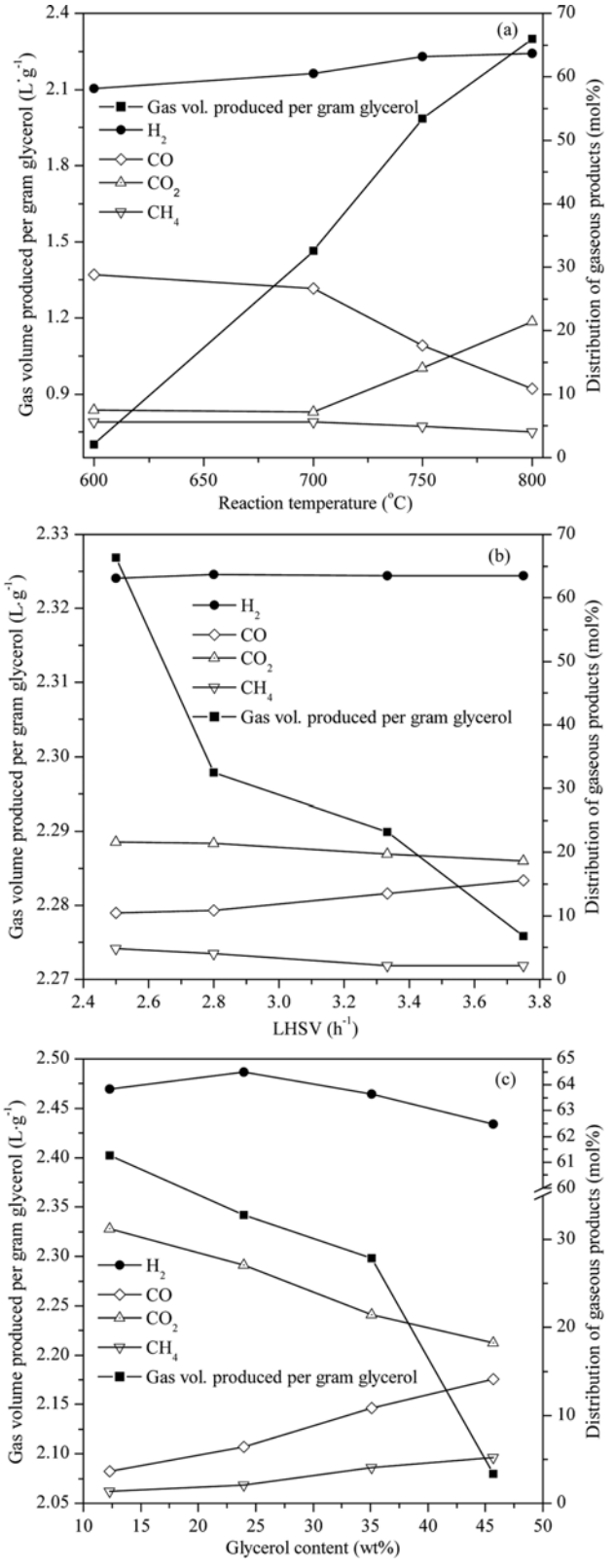

Fig. 6. Effect of reforming parameters on catalytic property of NiMoLa/CMA in GSR. Conditions: 15 ml catalyst and 100 ml·h^{-1} N_2 as balance gas are changeless, and (a) LHSV of 35 wt% glycerol aqueous solution 2.8 h^{-1}, (b) glycerol content in aqueous solution 35 wt% and reforming temperature 800 °C; (c) LHSV of glycerol aqueous solution 2.8 h^{-1} and reforming temperature 800 °C.

however, the formation of CO and CH_4 exhibits a diverse trend. A higher LHSV gives rise to a shorter contact time of glycerol, CO or CO_2 with the catalyst surface, which inhibits glycerol catalytic reforming to gas products and conversion of CO to CO_2 and H_2 through water-gas shift reaction.

Fig. 6(c) shows the effect of glycerol content in aqueous solution on the GSR over NiMoLaCMA. The results show that the conversion of unit glycerol to gaseous products and the production of H_2 and CO_2 decline with an increasing glycerol content. The increase of glycerol content leads to a decreasing steam content, which is disadvantageous to steam reforming and glycerol conversion. Additionally, the water-gas shift reaction also needs more water. Therefore, the further conversion of CO to CO_2 and H_2 can also be inhibited in the case of lower water content. However, the produced amount of CH_4 in gaseous products exhibits an increasing trend with the increasing glycerol content. It is perhaps because the higher glycerol content will lead to the production of more CO and H_2 instantaneously, which is helpful to the improvement on methanation through Eqs. (3) or (4) described in Scheme 1. From Fig. 6(c) a higher glycerol content in raw liquid is advantageous to GSR to syngas; however, a lower glycerol content can promote the water-gas shift reaction of CO to CO_2, which is helpful in the production of H_2 in GSR over NiMoLaCMA catalyst.

CONCLUSIONS

The presence of SMSI and acidic sites was disadvantageous to the improvement in the catalytic activity and catalytic stability of Ni-based catalysts supported γ-Al_2O_3 in GSR. The SMSI led to the formation of $NiAl_2O_4$. However, the Ni/γ-Al_2O_3 catalyst through the simultaneous modification of Mo, La, Ca and Mg (NiMoLa/CMA) remarkably exhibited an excellent catalytic stability in GSR to gaseous products such as H_2, CO and CO_2. A lower reforming temperature and a higher LHSV and glycerol content were helpful to the production of syngas from GSR over NiMoLa/CMA catalyst; the reverse conditions would improve the formation of H_2.

ACKNOWLEDGEMENTS

This work was supported by the Youth Science and Technology Foundation of Sichuan Province in China under Grant No. 2012 JQ0047.

REFERENCES

1. D. Roy, B. Subramaniam and R. V. Chaudhari, *Catal. Today*, **156**, 31 (2010).
2. Y. Nakagawa, Y. Shinmi, S. Koso and K. Tomishige, *J. Catal*., **272**, 191 (2010).
3. R. Sarkari, C. Anjaneyulu, V. Krishna and R. Kishore, *Catal. Commun*., **12**, 1067 (2011).
4. S. Dunn, *Int. J. Hydrog. Energy*, **27**, 235 (2002).
5. M. Asadullah, S. I. Ito, K. Kunimori, M. Yamada and K. Tomishige, *J. Catal*., **208**, 255 (2002).
6. D. A. Simonetti, E. L. Kunkes and J. A. Dumesic, *J. Catal*., **247**, 298 (2007).
7. E. L. Kunkes, D. A. Simonetti, J. A. Dumesic, W. D. Pyrz, L. E. Murillo, J. G. Chen and D. J. Buttrey, *J. Catal*., **260**, 164 (2008).
8. G. D. Wen, Y. P. Xu, H. J. Ma, Z. S. Xu and Z. J. Tian, *Int. J. Hydrog. Energy*, **33**, 6657 (2008).
9. K. Lehnert and P. Claus, *Catal. Commun*., **9**, 2543 (2008).
10. D. Karthikeyan, G. S. Shin, D. J. Moon, J. H. Kim, N. C. Park and Y. C. Kim, *J. Nanosci. Nanotechnol*., **11**, 1443 (2011).
11. A. J. Byrd, K. K. Pant and R. B. Gupta, *Fuel*, **87**, 2956 (2008).
12. J. H. Sinfelt and D. J. C. Yates, *J. Catal*., **8**, 82 (1967).
13. F. Mariño, M. Boveri, G. Baronetti and M. Laborde, *Int. J. Hydrog. Energy*, **26**, 665 (2001).
14. J. da S. Lisboa, D. C. R. M. Santos, F. B. Passos and F. B. Noronha, *Catal. Today*, **101**, 15 (2005).
15. M. C. Sánchez-Sánchez, R. M. Navarro and J. L. G. Fierro, *Int. J. Hydrog. Energy*, **32**, 1462 (2007).
16. I. Suelves, M. I. Lazaro, R. Moliner, Y. Echegoyen and J. M. Palacios, *Catal. Today*, **116**, 271 (2006).
17. S. S. Maluf and E. M. Assaf, *Fuel*, **88**, 1547 (2009).
18. M. H. Youn, J. G. Seo, P. Kim and I. K. Song, *J. Mol. Catal. A*, **261**, 276 (2007).
19. T. Huang, W. Huang, J. Huang and P. Ji, *Fuel Process. Technol*., **92**, 1868 (2011).
20. F. Barath, M. Turki, V. Keller and G. Maire, *J. Catal*., **185**, 1 (1999).
21. T. Valliyappan, D. Ferdous, N. N. Bakhshi and A. K. Dalai, *Top Catal*., **49**, 59 (2008).
22. D. C. Rennard, J. S. Kruger and L. D. Schmidt, *ChemSusChem*., **2**, 89 (2009).
23. S. Y. Park, J. H. Kim, D. J. Moon, N. C. Park and Y. C. Kim, *J. Nanosci. Nanotechnol*., **10**, 3175 (2010).